Received: 1 March 2019 | Revised: 1 June 2020 | Accepted: 4 June 2020

DOI: 10.1002/glia.23874

GLIA

WILEY

RESEARCH ARTICLE

Glial glutamate transporter GLT-1 determines susceptibility to spreading depression in the mouse cerebral cortex

Hidenori Aizawa[1,2] | Weinan Sun[1] | Kaori Sugiyama[1] | Yukiko Itou[1] | Tomomi Aida[1] | Wanpeng Cui[1,2] | Saori Toyoda[1] | Haruhi Terai[2] | Michiko Yanagisawa[1] | Kohichi Tanaka[1,3]

[1]Laboratory of Molecular Neuroscience, Medical Research Institute, Tokyo Medical and Dental University, Tokyo, Japan

[2]Department of Neurobiology, Graduate School of Biomedical and Health Sciences, Hiroshima University, Hiroshima, Japan

[3]Center for Brain Integration Research, Tokyo Medical and Dental University, Tokyo, Japan

Correspondence
Hidenori Aizawa, Department of Neurobiology, Graduate School of Biomedical and Health Sciences, Hiroshima University, 1-2-3 Kasumi, Minami-ku, Hiroshima 734-8553, Japan.
Email: haizawa@hiroshima-u.ac.jp

Funding information
Japan Agency for Medical Research and Development, Grant/Award Number: JP18dm0107093h0003; Core Research for Evolutional Science and Technolo of Japan Science and Technology Agency, Grant/Award Numbers: KAKENHI-JP17K19459, KAKENHI26112010; Ministry of Education, Culture, Sports, Science and Technology, Grant/Award Number: JP19H05723

Abstract

Cortical spreading depression (CSD) is a pathological neural excitation that underlies migraine pathophysiology. Since glutamate receptor antagonists impair CSD propagation, susceptibility to CSD might be determined by any of the neuronal (excitatory amino acid carrier 1 [EAAC1]) and glial (GLutamate ASpartate Transporter [GLAST] and glial glutamate transporter 1 [GLT-1]) glutamate transporters, which are responsible for clearing extracellular glutamate. To investigate this hypothesis, we performed electrophysiological, hemodynamic, and electrochemical analyses using EAAC1- (EAAC1 KO), GLAST- (GLAST KO), and conditional GLT1-1-knockout mice (GLT-1 cKO) to assess altered susceptibility to CSD. Despite the incomplete deletion of the gene in the cerebral cortex, GLT-1 cKO mice exhibited significant reduction of GLT-1 protein in the brain without apparent alteration of the cytoarchitecture in the cerebral cortex. Physiological analysis revealed that GLT-1 cKO showed enhanced susceptibility to CSD elicited by chemical stimulation with increased CSD frequency and velocity compared to GLT-1 control. In contrast, the germ-line EAAC1 and GLAST KOs showed no such effect. Intriguingly, both field potential and cerebral blood flow showed faster dynamics with narrower CSD than the controls. An enzyme-based biosensor revealed more rapid accumulation of glutamate in the extracellular space in GLT-1 cKO mice during the early phase of CSD than in GLT-1 control, resulting in an increased susceptibility to CSD. These results provided the first evidence for a novel role of GLT-1 in determining susceptibility to CSD.

KEYWORDS

astrocytes, glutamate, glutamate transporters, migraine, spreading depression

1 | INTRODUCTION

Spreading depression is a propagating wave of membrane depolarization that occurs in neuronal and glial cells (Lauritzen, 1994). Recently, this pathological excitation of the brain has attracted increasing interest following imaging studies showing an association between cortical spreading depression (CSD) and neurological disorders such as migraine (Dreier, 2011). Despite the clinical significance of CSD, molecular mechanisms that regulate the brain's susceptibility to CSD remain unclear.

During CSD generation, the excitatory neurotransmitter glutamate is released from the presynaptic axonal terminal into the

Hidenori Aizawa and Kohichi Tanaka should be considered joint senior author.

synaptic cleft via neuronal stimulation or energy failure due to hypoxia (Somjen, 2001). Glutamate might also play a critical role in CSD generation, since blocking the *N*-methyl-D-aspartate glutamate receptor attenuated the negative shift of extracellular field potential associated with CSD (Lauritzen & Hansen, 1992).

Since the concentration of extracellular glutamate is regulated via glutamate transporters expressed in neurons and glial cells (Danbolt, 2001), reduced activity of any of these transporters is a primary candidate mechanism for determining the cellular susceptibility to CSD. Indeed, a recent study found that a nonspecific glutamate transporter blocker enhanced the velocity of CSD propagation in vitro (Zhou et al., 2013).

Three glutamate transporter genes are expressed in the mammalian forebrain: excitatory amino acid carrier 1 [EAAC1], also known as EAAT3) (Kanai & Hediger, 1992), GLAST (GLutamate ASpartate Transporter, also known as EAAT1) (Storck, Schulte, Hofmann, & Stoffel, 1992; Tanaka, 1993), and glial glutamate transporter 1 (GLT-1) also known as EAAT2) (Pines et al., 1992). In adult rat brain, GLAST and GLT-1 are expressed primarily in astrocytes, while EAAC1 is highly expressed in neuron (Rothstein et al., 1994). Although perturbing these glutamate transporters had profound effects on neural excitability such as lethal seizure (Sugimoto et al., 2018; Tanaka, 1997), it remains elusive which glutamate transporter specifically affects the susceptibility of brain to CSD. Thus, identifying the specific glutamate transporter gene(s) involved with CSD generation is essential for developing novel diagnostic and therapeutic strategies for associated disorders. To address this, we performed electrophysiological, hemodynamic, and electrochemical analyses in mice lacking the genes encoding GLAST, GLT-1, or EAAC1 to reveal the respective effects on susceptibility to CSD.

2 | MATERIALS AND METHODS

2.1 | Animals

All experiments were performed in accordance with the Animal Experiment Plan (0140127A) and Recombinant DNA Experiment Plan (2012-003C17) approved by the Animal Experiment Committee and Recombinant DNA Experiment Committee of Tokyo Medical and Dental University, respectively. Mice were maintained throughout the experiments on a 12 hr light/dark cycle.

GLAST$^{-/-}$ and EAAC1$^{-/-}$ mice were obtained from their heterozygote breeder pairs with disrupted Exon 6 of murine GLAST (Watase et al., 1998) and Exon 1 of murine EAAC1 (Peghini, Janzen, & Stoffel, 1997), respectively. The Tg(hGFAP-Cre) transgenic line (Bajenaru et al., 2002) and floxed-GLT-1 (GLT-1$^{flox/+}$) line (Cui et al., 2014; Zhao, Hiraoka, Ogawa, & Tanaka, 2018), in which Exon 4 was flanked by two loxP elements in Introns 3 and 4, were used. GLT-1 conditional KO mice were siblings generated by crossing Tg(hGFAP-Cre$^{+/-}$); GLT-1$^{flox/+}$; and GLT-1$^{flox/flox}$ (Figure 1a). Heterozygotes of all of these mutants were outbred to the wild-type C57BL6J mouse strain for more than six generations before this study. We chose hGFAP-Cre; GLT-1$^{flox/+}$ heterozygous mice as control, because it had a closer genetic background to the hGFAP-Cre; GLT-1$^{flox/flox}$ homozygous mice of our interest.

For electrical, hemodynamic, and glutamate measurement during CSD, we used 12 to 24-week-old male mice. We analyzed changes in body weight and survival rate using both male and female littermates.

2.2 | Measurement of blood pressure and heart rate

Heart rate and blood pressures were measured in awake 9-week-old mice using noninvasive blood pressure analysis system (BP-98A, Sorton) according to the manufacturer's instruction.

2.3 | Western blot analysis

Quantitative analysis of the GLT-1 protein expressed in the brain of GLT-1$^{flox/flox}$ and Tg(hGFAP:Cre); GLT-1$^{flox/flox}$ mice (N = 3) were performed as described previously (Aida et al., 2015). Briefly, whole brain were dissected from the mice sacrificed with pentobarbital (100 mg/kg, i.p.) and homogenized in lysis buffer (20 mM Tris–HCl, pH 7.4; 0.32 M sucrose and Complete Protease Inhibitor Cocktail tablet [Roche Diagnostics]). After sonication, protein concentration was determined by BCA Assay (Sigma, St. Luis, MO), and samples were diluted with equal amounts of 2× sample buffer (250 mM Tris–HCl, pH 6.8; 4% SDS; 10% glycerol; and 1% β-mercaptoethanol). After denaturation by heating at 95°C for 10 min, 10 μg of each sample was separated by 12% SDS-PAGE along with a protein standard ladder (Blue Star, Nippon Genetics, Tokyo, Japan). The samples were then transferred to PVDF membranes (Millipore) and blocked in TBS with 0.2% Tween 20 (TBS-T) and 5% skim milk for 1 hr at room temperature. Membranes were then incubated with primary antibodies in TBS-T containing 1% skim milk at 4°C overnight. Next, the membranes were washed, incubated with HRP-conjugated secondary antibodies at room temperature for 1 hr, washed, and visualized with Luminata Forte Western HRP substrate (Millipore). Gel images were taken every 6 s for 10 min using Image Lab software (Bio-Rad). The following antibodies were used: rabbit polyclonal anti-GLT-1 (1:5,000, a gift from M. Watanabe, Hokkaido University) (Tanaka, 1997); anti-GLAST (1:2,500, a gift from M. Watanabe, Hokkaido University) (Watase et al., 1998); polyclonal anti-EAAC1 (1:500, Santa Cruz Biotechnology, Santa Cruz, CA, sc-25658); mouse monoclonal anti-β-actin (1:5,000, Santa Cruz Biotechnology, sc-47778); HRP-conjugated anti-rabbit IgG (1:10,000, Jackson ImmunoResearch Laboratories, West Grove, PA, 711-035-152); and HRP-conjugated anti-mouse IgG (1:10,000, Jackson ImmunoResearch Laboratories, 715-035-151). Band intensities of gel images within linear signal range were quantified using Image Lab software and normalized with band intensities of β-actin.

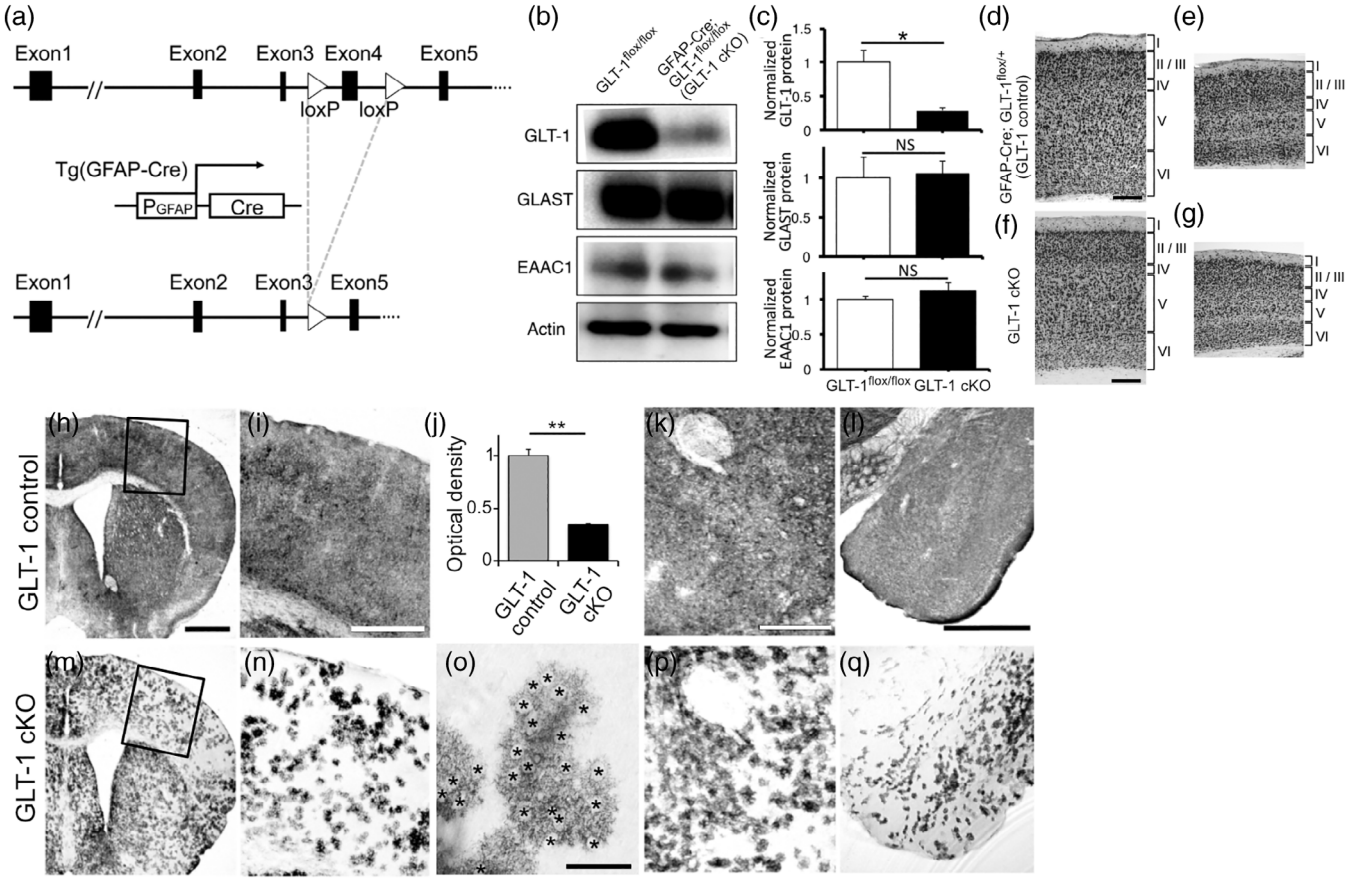

FIGURE 1 Generation of the conditional knockout mouse for GLT-1. (a) Schematic diagram showing the strategy for generating the Tg(hGFAP-Cre); GLT-1$^{flox/flox}$ (GLT-1 cKO), in which the GLT-1 gene is defective only in the astrocytes expressing Cre recombinase under control of the human GFAP promoter (P_{GFAP}). Exon 4 of the GLT-1 gene encodes the transmembrane domain, which is essential for transporter activity. (b) Western blot analysis of GLT-1, GLAST EAAC1, and β-actin of the whole brain from GLT-1$^{flox/flox}$ and GLT-1 cKO mice. (c) Bar plot showing GLT-1 (top), GLAST (middle), and EAAC1 (bottom) band intensities normalized with those of β-actin (N = 3–6 for each group). Data are presented as the mean ± *SEM*. Asterisk indicates a significant difference with $p < .05$ in Student's t test. NS, not significant. (d–g) Coronal sections of the primary motor cortex (d,f) and the primary visual cortex (e,g) of Tg(hGFAP-Cre); GLT-1$^{flox/+}$ (GLT-1 control in (d,e)) and Tg(hGFAP-Cre); GLT-1$^{flox/flox}$ mice (GLT-1 cKO in (f,g)) showing NeuN immunoreactivity. (h,i,k–q) Coronal sections of the primary motor cortex (h,i,m,n,o), ventral striatum (k,p), and amygdala (l,q) of GLT-1 control (h,i,k,l) and GLT-1 cKO mice (m–q) showing GLT-1 immunoreactivity. Panel (o) is high magnification view of the boxed areas in (n). Asterisks in (o) indicate the cell bodies of the presumptive neurons. (j) A bar graph showing the optical density of the GLT-1 immunoreactivity in GLT-1 control and GLT-1 cKO mice. Values are represented as means ± *SEM*. Scale bars, 1 mm in (h) (applies to (m)), 500 μm in (i) (applies to (n)), 200 μm in (d) (applies to (f)) and (e) (applies to (g)), and 50 μm in (o). EAAC1, excitatory amino acid carrier 1; GLAST, GLutamate ASpartate Transporter; GLT-1, glial glutamate transporter 1

2.4 | Recording extracellular field potential and cerebral flood flow during CSD

Animals were anesthetized by urethane (1.4 g/kg, i.p.) and placed in a stereotaxic apparatus (SR-8N, Narishige, Tokyo, Japan). Body temperature was monitored and retained with a heating pad (BWT-100A, Bio Research Center Co. Ltd., Nagoya, Japan). A glass capillary (1–2 MΩ) filled with 0.5 M NaCl was placed 0.2 mm beneath the brain surface into the posterior primary motor cortex (Rec1 in Figure 2b, 1.0 mm posterior and 1.0 mm lateral to the bregma) and the anterior secondary motor cortex (Rec2 in Figure 2b, 1.0 mm anterior and 1.0 mm lateral to the bregma) (Paxinos & Franklin, 2008). Extracellular potential was recorded with an Ag/AgCl reference electrode placed on the nose bone. Direct current (DC) potentials were amplified (EX4-400, Dagan Corporation, Minneapolis, MN) and sampled at 1 kHz (Powerlab, ADInstruments, Dunedin, New Zealand). In some experiments, changes in cerebral blood flow (CBF) associated with CSD were recorded simultaneously by measuring extracellular field potential using a laser Doppler probe (ALF21, Advance Co., Ltd., Tokyo, Japan) placed in Rec1 (Figure 2a). A cotton ball soaked in 300 mM KCl solution was applied to the visual cortex (2 mm lateral and 0 mm anterior to the lambda) to induce CSD (black arrow in Figure 2a). We replaced the cotton ball every 15 min to maintain the KCl concentration during recording, which lasted more than 60 min.

2.5 | Glutamate measurement using an enzyme-based biosensor

A custom-made electrode comprising a platinum-iridium working electrode of 250 μm in diameter coated with a thin layer of glutamate

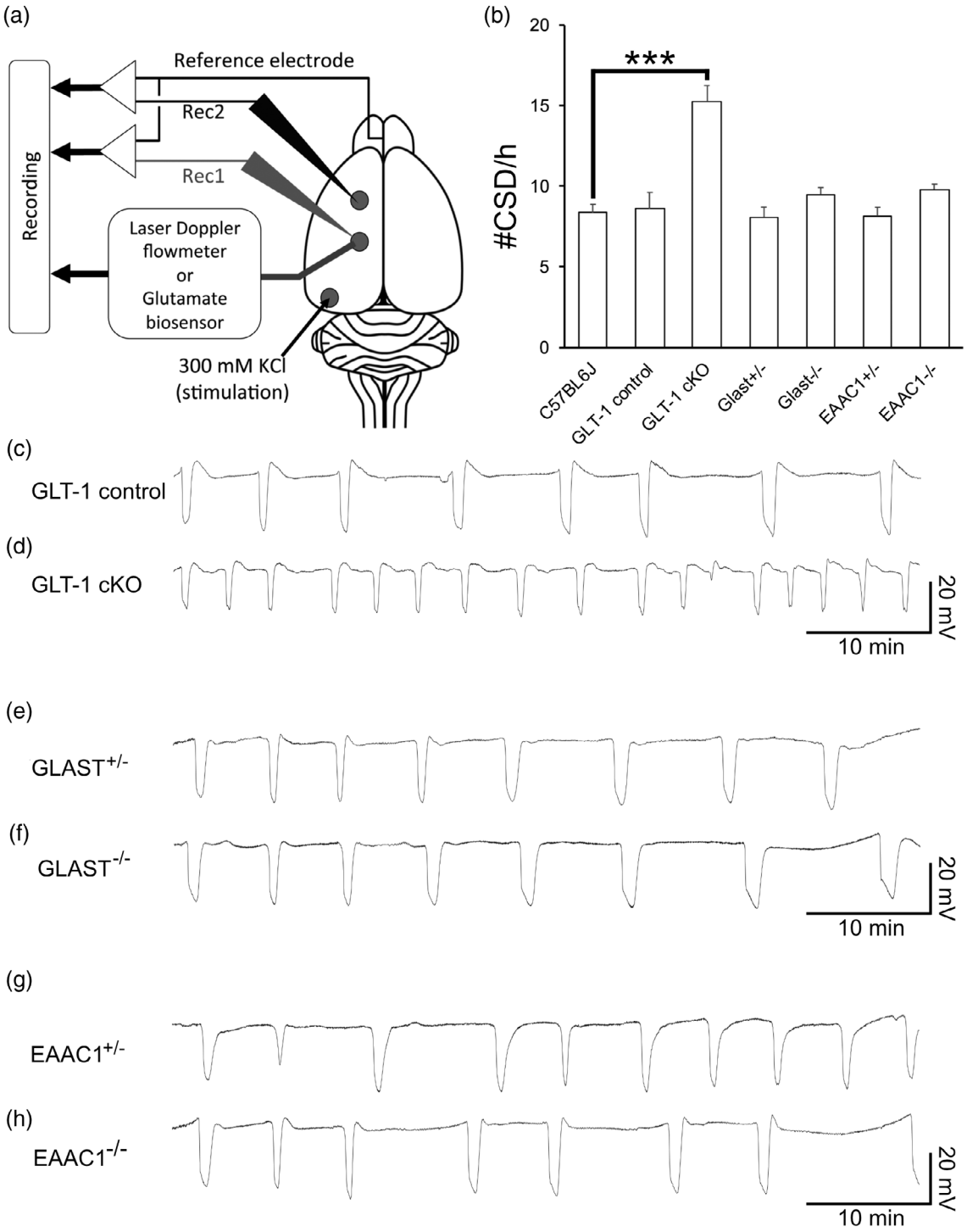

FIGURE 2 GLT-1 conditional knockout mouse showed increased susceptibility to the CSD. (a) Schematic diagram of the dorsal view of mouse brain showing the position of the electrodes for DC potential recording (Rec1 and Rec2), cerebral blood flow (laser Doppler flowmeter), or glutamate biosensor. (b) A bar graph showing mean numbers of the CSD in an hour in the wild-type (C57BL6J) and six mutants. Values are represented as means ± *SEM*. Triple asterisks, $p < .001$ in Tukey's post hoc analysis following one-way ANOVA. (c–h) Representative raw traces of the DC potential changes during spreading depression in GLT-1 control (c), GLT-1 cKO (d), GLAST$^{+/-}$ (e), GLAST$^{-/-}$ (f), EAAC1$^{+/-}$ (g), and EAAC1$^{-/-}$ (h). ANOVA, analysis of variance; CSD, cortical spreading depression; DC, direct current; EAAC1, excitatory amino acid carrier 1; GLAST, GLutamate ASpartate Transporter; GLT-1, glial glutamate transporter 1

oxidase was integrated with the Ag/AgCl reference electrode (Pinnacle technology, Inc., Lawrence, KS) to create a biosensor for glutamate measurements (Hu, Mitchell, Albahadily, Michaelis, & Wilson, 1994). The minimal distance between working and reference electrodes was 300 μm. The biosensor was initially calibrated in vitro using an increasing concentration of L-glutamate (072-00501, Wako Pure Chemical

Industries, Ltd., Osaka, Japan) from 10 to 50 μM in a two-layered chamber whose outer jacket was perfused with water preheated to 37°C. Then, we placed the biosensor and glass electrode at the posterior primary motor cortex (at the same coordinate as described above) to measure extracellular glutamate and DC potential, respectively. We elicited CSD to measure glutamate concentration as described above. The biosensor was used for amperometry by applying a +0.6-V potential through a potentiostat (Model 3104, Pinnacle Technology Inc.). Signals for DC potential and extracellular glutamate were simultaneously sampled at 1 and 4 Hz, respectively (Powerlab, ADInstruments).

2.6 | Histology

Animal was deeply anesthetized with urethane (1.6 g/kg, i.p.) and fixed by transcardiac perfusion of 4% paraformaldehyde in 0.1 M phosphate-buffered saline (pH 7.4, PBS). Removed brain was further fixed by immersion in the same fixative overnight. Then, 50-μm-thick sections (100 μm apart) were cut by freezing microtome and processed for immunohistochemistry. After three washes in PBS, free-floating sections were incubated in 1% blocking reagent (11096176001, Roche Diagnostics GmbH, Mannheim, Germany) containing polyclonal rabbit anti-GLT-1 (1:2,000 dilution, a gift from Professor Watanabe from Hokkaido University), or monoclonal mouse anti-NeuN antibody (1:500 dilution, MAB377, Millipore, Billerica, MA) at 4°C overnight. The sections were again washed three times in PBS, and then incubated in goat anti-rabbit IgG conjugated with biotin (1:1,000, BA-1000, Vector Laboratories Inc., Burlingame, CA) or goat anti-mouse IgG conjugated with biotin (1:1,000, BA-9200, Vector Laboratories Inc.) at room temperature for 2 hr. After three final washes in PBS, the antibody binding was visualized using the avidin–biotin–peroxidase complex (VECTASTAIN Elite ABC, Vector Laboratories Inc.) with diaminobenzidine and nickel. Some sections were counter-stained with Neutral Red. For quantification of GLT-1 immunoreactivity, images were acquired by charge coupled device camera attached to the compound microscope (BX51, Olympus). Relative optical density was measured in area of 300 μm × 300 μm in the primary motor cortex using ImageJ (http://rsb.info.nih.gov/ij/).

2.7 | Data analysis

The extracellular field potential data were analyzed by custom-written scripts in MATLAB (MathWorks, Natick, MA). After importing the data, signals were downsampled to 100 Hz and filtered using a Butterworth filter with a bandwidth of 0.001–0.1 Hz. By detecting the negative peak of the DC potential during CSD, we calculated the following parameters: the number of CSD in an hour after the onset of KCl application, interval between CSDs, and amplitudes and durations of the negative shift of DC potential during CSD. For the amplitude, we first detected the first (p1) and second positive peaks (p2) flanking the negative peak of DC shift (n1), and then calculated the length of the perpendicular line drawn from n1 to the line connecting p1 and p2 as amplitude. Duration was the width of CSD at half of the maximal amplitude. To determine the velocity of CSD propagation, the onset of CSD was represented as the time at which the slope of the descending phase of CSD was steepest. Velocity was then calculated by dividing the constant distance between electrodes by the time elapsed for CSD to propagate from Rec1 to Rec2 (Figure 2b).

For CBF, signal was converted to the percentage change from the baseline calculated from the 30-s recording before chemical stimulation. We detected the onset and peak of transients in both CBF and extracellular glutamate concentration as the local minimum and maximum of the signals, respectively. We excluded change in the CBF during the first CSD showing a multiphase response, which is reportedly characteristic of the first, but not subsequent, CSDs (Yuzawa et al., 2012).

Data were analyzed statistically by two-tailed *t* test (two groups data), one-way analysis of variance followed by Tukey's multiple comparison (for more than three groups data), log-rank test (survival rate analysis), Pearson's correlation using GraphPad Prism 4 (Graphpad Software Inc., San Diego, CA), and Jamovi version 1.2 (https://www.jamovi.org).

3 | RESULTS

3.1 | Generation of the conditional GLT-1 knockout mice

To test whether the glutamate transporters expressed in the forebrain play a role in regulating CSD susceptibility, we used mice defective in EAAC1, GLT-1, or GLAST activity.

We generated a mouse lacking GLT-1 gene expression in only a subpopulation of astrocytes by using a floxed-GLT-1 mutant mouse in which Exon 4 of the murine GLT-1 genes was flanked by two loxP elements (Figure 1a). By crossing this line with Tg(hGFAP-Cre) mice expressing Cre recombinase also in an astrocyte subpopulation (Bajenaru et al., 2002), we generated the GLT-1 conditional knockout mice, hGFAP-Cre; GLT-$1^{flox/flox}$ (hereafter, GLT-1 cKO) and hGFAP-Cre; GLT-$1^{flox/+}$ (hereafter, GLT-1 control).

At 62 days of age, 66.7% of GLT-1 cKO (N = 14) mice remained alive, compared to less than 40% of germ-line GLT-1 knockout mice (Tanaka, 1997). None of the GLT-1 control animals died during analysis (N = 8), and a log-rank test for statistical differences in survival rate detected no significant difference between groups (χ^2 = 2.573, p = .109), suggesting that a substantial portion of the GLT-1 cKO mouse line grew to adulthood. Thus, we could examine the influence of GLT-1 deletion on CSD in adult brain.

Western blot analysis revealed that the GLT-1 cKOs showed significant reduction of GLT-1 protein expression in the brain to the 28.7% of GLT-$1^{flox/flox}$ mice (N = 3 for each group, p = .0185) (Figure 1b,c). None of the other glutamate transporters GLAST and EAAC1 showed significant changes in their protein expression in the brain (N = 5 for each group; p = .950 for GLAST vs. GLT-$1^{flox/flox}$; p = .698; Figure 1b,c), suggesting the lack of apparent compensation of reduced GLT-1 function by overexpression of those transporters

protein. We did not observed significant alterations in cytoarchitecture in any forebrain region including primary motor (Figure 1d,f) and visual cortices (Figure 1e,g) of the GLT-1 cKO, as revealed by expression of the neuronal marker NeuN.

The GLT-1 cKO mice exhibited reduction of GLT-1 immunoreactivity, with patchy expression patterns observed in all forebrain regions such as cerebral cortex (Figure 1m,n), striatum (Figure 1p), amygdala (Figure 1q), and hippocampus (data not shown), compared to the ubiquitous expression of GLT-1 in GLT-1 control (Figure 1h,i,k, l). Examination at higher magnification localized the GLT-1 immunoreactivity to the fine and short cellular processes (Figure 1o), suggesting that the majority of the cells expressing GLT-1 in GLT-1 cKO mice were with astrocyte-like morphology. Quantification of the GLT-1-expressing cells based on optical density of the immunoreactivity revealed that GLT-1 cKO showed significantly reduction of immunoreactivity over the GLT-1 control (Figure 1j, $p = .003$, $N = 6$ mice).

These results indicated that, despite the loss of GLT-1 in a substantial number of cells, GLT-1 cKOs grew to adulthood, enabled further investigation of CSD in adult brain.

All homozygotes for the EAAC1 and GLAST knockout alleles also survived to adulthood ($N = 6$ for both) (Peghini et al., 1997; Watase et al., 1998).

3.2 | Reduction in GLT-1, but not EAAC1 or GLAST, activity led to an increased susceptibility to CSD

To examine the direct influence of defects in glutamate transporter activity on CSD, we recorded the DC potential in the posterior primary (Rec1 in Figure 2a) and anterior secondary motor cortices (Rec2 in Figure 2a) of the mutants lacking glutamate transporter genes. CSD was elicited by topical application of KCl to the visual cortex (Figure 2a). The number of CSD induced within an hour was used to indicate the susceptibility of brain to CSD, based on previous studies (Ayata, 2013). As compared to the C57BL6J, we observed that only the GLT-1 cKO showed significantly more frequent CSDs among mutants (Figure 2b, $p < .001$).

Specifically, The GLT-1 cKO mice showed more frequent and faster CSD (Figure 2d) than GLT-1 control (Figure 2c). Quantitative analysis corroborated this finding showing an increased velocity ($p = .0372$), larger number of CSDs per hour ($p = .0009$), and shortened inter-CSD intervals ($p = .0075$) compared to GLT-1 control (Table 1), suggesting increased susceptibility in the GLT-1 cKOs to CSD.

These electrophysiological measures of CSD in GLAST$^{-/-}$ (Figure 2f) and EAAC1$^{-/-}$ mice (Figure 2h) were comparable with those of the control groups (Figure 2e,g), and showed no statistically significant differences (Table 1).

These results suggested that GLT-1, but not EAAC1 or GLAST, plays a critical role in determining the susceptibility of mouse forebrain to CSD.

3.3 | Reduced GLT-1 affected the neurovascular dynamics during CSD

Depolarization of neuronal and glial cells during CSD in mouse has been coupled to changes in metabolic and hemodynamic activity (Ayata et al., 2004). Therefore, to ascertain the effect of GLT-1 deletion on these changes during CSD, we performed laser Doppler flowmetry to measure CBF simultaneously with negative shifts in DC potential. Consistent with a previous study (Ayata et al., 2004), we observed transient increases in the CBF (Figure 3c,d) in association with negative shifts in DC potential (Figure 3a,b) in the posterior primary motor cortex of GLT-1 control ($N = 5$) and GLT-1 cKO ($N = 7$), while the visual cortex was continuously stimulated with KCl. Intriguingly, we found that the negative shifts in DC potential were of shorter duration in GLT-1 cKOs compared to GLT-1 controls ($p = .0027$) (Table 1), without significant changes observed in the amplitude during CSD ($p = .395$) (Table 1). This was coupled to the shorter CBF duration in GLT-1 cKOs ($N = 11$) compared to GLT-1 controls ($N = 6$ mice, $p = .0138$) (Figure 3f). The effect of GLT-1 deletion on CSD shape could not be attributed to an impairment of systemic blood pressure or local vascular response, since GLT-1 cKOs showed blood pressure (systolic, $p = .991$; diastolic, $p = .771$) (black in

TABLE 1 Electrophysiological measurements of the CSD in mutants lacking glutamate transporters

	N	Interval (s)	Amplitude (mV)	Velocity (mm/min)	Duration at half amplitude (s)
GLT-1 control	5	385.00 ± 45.14	18.45 ± 0.77	3.62 ± 0.09	52.73 ± 3.24
GLT-1 cKO	7	242.36 ± 17.27	16.39 ± 1.86	5.64 ± 0.70	32.77 ± 3.15
		($p < .01$)		($p < .05$)	($p < .01$)
Glast$^{+/-}$	9	340.12 ± 24.58	20.88 ± 1.11	4.34 ± 0.15	50.35 ± 2.43
Glast$^{-/-}$	6	389.81 ± 45.44	18.08 ± 0.86	4.53 ± 0.15	48.77 ± 5.94
EAAC1$^{+/-}$	6	354.43 ± 22.72	19.33 ± 2.84	3.94 ± 0.34	45.99 ± 2.89
EAAC1$^{-/-}$	6	395.97 ± 51.90	23.44 ± 1.25	4.17 ± 0.34	38.91 ± 2.53

Note: Values are represented as means ± *SEM*.

Abbreviations: CSD, cortical spreading depression; EAAC1, excitatory amino acid carrier 1; GLAST, GLutamate ASpartate Transporter; GLT-1, glial glutamate transporter 1.

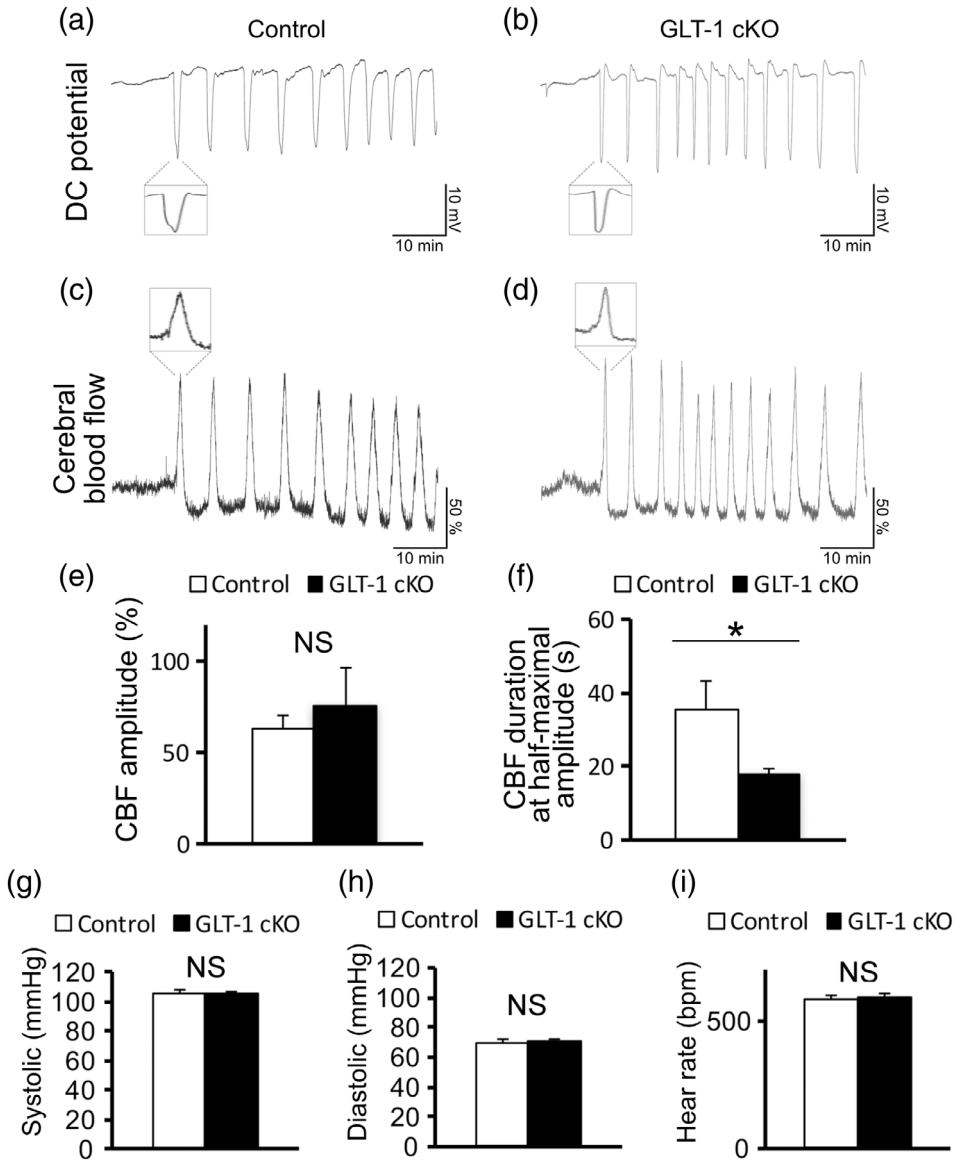

FIGURE 3 Faster response of the regional CBF during CSD in GLT-1 cKO. (a–d) Simultaneous measurement of DC potential (a,b) and CBF (c,d) during CSD in GLT-1 control (a,c) and GLT-1 cKO (b,d) mouse. Insets are magnified view of the first CSD in each record. (e,f) Bar graphs showing mean values of the amplitude (e) and width at half-maximal amplitude (f) of changes in CBF associated with CSD in GLT-1 control (white) and GLT-1 cKO (black). (g–i) Bar graphs showing mean values of the systemic blood pressure (systolic and diastolic in (g) and (h), respectively) and heart rate in immobilized GLT-1 control (white) and GLT-1 cKO mice (black). Error bars, *SEM*. NS, not significant. Asterisk indicates a significant difference with $p < .05$ in Student's *t* test. ANOVA, analysis of variance; CSD, cortical spreading depression; DC, direct current; EAAC1, excitatory amino acid carrier 1; GLAST, GLutamate ASpartate Transporter; GLT-1, glial glutamate transporter 1

Figure 3g,h), heart rate ($p = .789$) (black in Figure 3i) and CBF amplitude ($p = .487$) (black in Figure 3e) comparable to those in GLT-1 controls (white in Figure 3e,g–i).

These results suggested that reducing glutamate transporter activity via GLT-1 deletion enhances the dynamics in cellular membrane potential and vascular response.

3.4 | Impaired activity of glutamate transporter GLT-1 induced faster changes in the extracellular glutamate concentration during CSD

In the resting state, glial cells uptake extracellular glutamate, while after depolarization they release glutamate to the extracellular space by reversed electrogenic uptake (Phillis, Ren, & O'Regan, 2000; Rossi, Oshima, & Attwell, 2000; Szatkowski, Barbour, & Attwell, 1990). Since GLT-1 expressed in astrocytes uptakes more than 90% of the extracellular glutamate in forebrain (Haugeto et al., 1996; Tanaka, 1997), we hypothesized that impairment of GLT-1 would affect the extracellular field potential and CBF during CSD by altering the dynamics of glutamate in the extracellular space.

To address this, we used a glutamate biosensor comprising a platinum-iridium electrode coated with a thin layer of glutamate oxidase. In the presence of glutamate, glutamate oxidase generates hydrogen peroxide, which is detected as oxidative current by the platinum-iridium electrode (Hu et al., 1994) (Figure 4a). Recording with this electrode showed instantaneous changes in current in response to the increased glutamate concentration in vitro (Figure 4b). Such current changes measured using the biosensor were significantly correlated with glutamate concentration ($R^2 = .668$, $p = 3.606 \times 10^{-19}$, $N = 15$ electrodes) (Figure 4c), suggesting that this technique allowed us to measure the glutamate concentration with fine temporal resolution. Indeed, with the electrode placed in the posterior primary motor cortex of the wild-type mouse, we observed

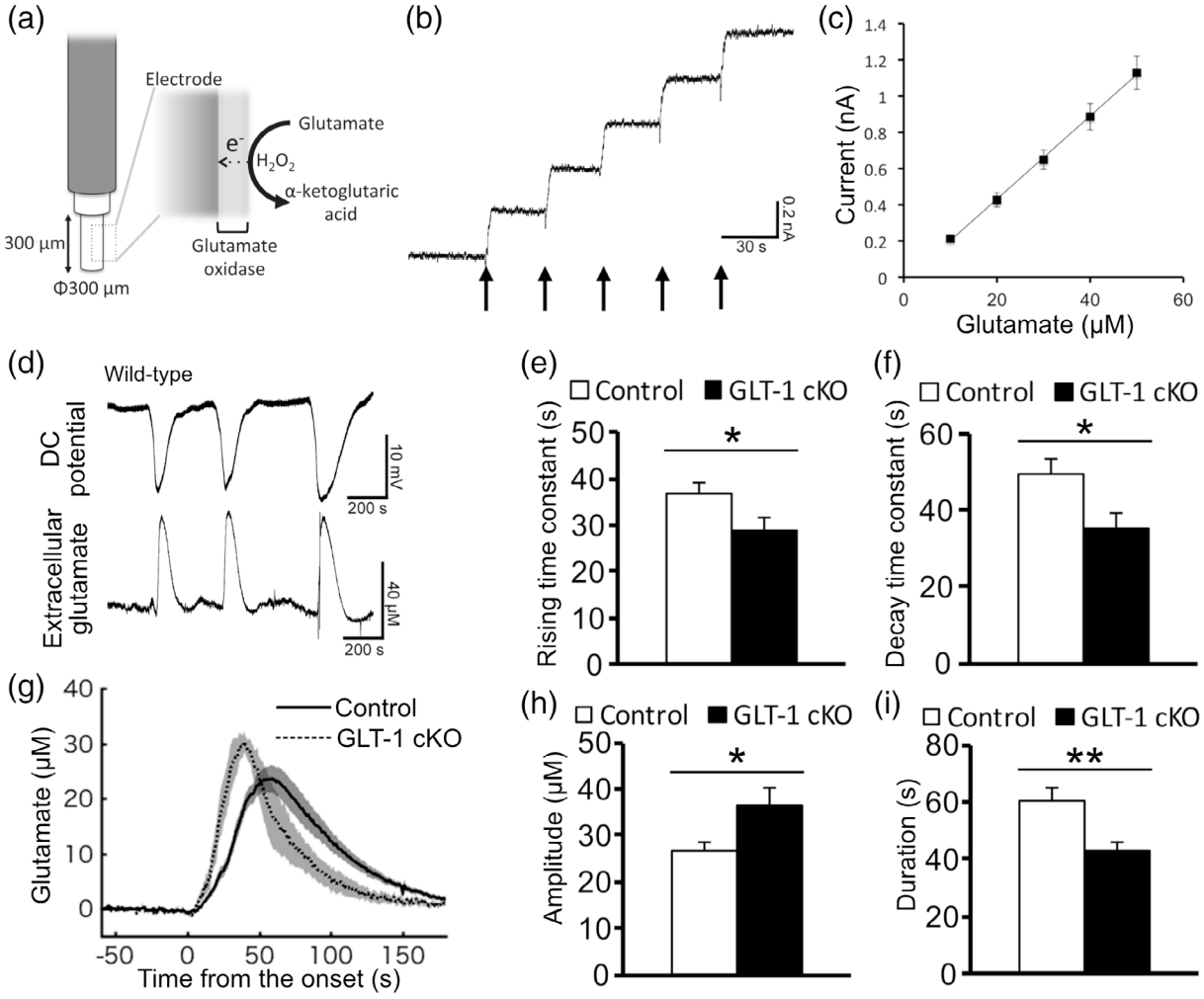

FIGURE 4 GLT-1 deletion affected the susceptibility to CSD via altered dynamics in extracellular glutamate. (a) Schematic diagram of a platinum electrode (dark gray) coated with a layer of glutamate oxidase (light gray) showing the principle of measuring extracellular glutamate concentration electrochemically. (b) Line plot of the current recorded by glutamate biosensor during the in vitro calibration. Glutamate concentration increased by 10 µM every 30 s as indicated by black arrows. (c) Line plot showing mean values of the current amplitude in response to the changes in glutamate concentration in vitro. (d) Raw traces of DC potential (upper trace) and extracellular glutamate concentration (lower trace) recorded simultaneously during CSD in a wild-type mouse. (g) Line plots of the mean value of glutamate concentration in GLT-1 control (solid line) and GLT-1 cKO mice (dashed line) aligned with the onset of CSD. (e,f,h,i) Bar graphs showing mean values of rising (e) and decaying time constants (f), amplitude (h), and duration (i) of extracellular glutamate concentration during CSD in GLT-1 control (white) and GLT-1 cKO mice (black). Error bars and shaded areas indicate the *SEM*. Single and double asterisks indicate significant difference with $p < .05$ and $p < .01$ in Student's *t* test, respectively. ANOVA, analysis of variance; CSD, cortical spreading depression; DC, direct current; EAAC1, excitatory amino acid carrier 1; GLAST, GLutamate ASpartate Transporter; GLT-1, glial glutamate transporter 1

transient increases in glutamate concentration (bottom trace in Figure 4d) in close temporal association with negative shifts in DC potential recorded by the glass pipette placed in the same cortical areas (top trace in Figure 4d).

Extracellular glutamate concentration in the posterior primary motor cortex following the application of KCl in the visual cortex increased more rapidly in the GLT-1 cKO mice ($N = 5$, dashed line in Figure 4g) than in GLT-1 control ($N = 11$, solid line in Figure 4g) as revealed by the shorter rising time constant in GLT-1 cKOs (black in Figure 4e) compared to GLT-1 controls ($p = .037$) (white in Figure 4e). Consistent with this, amplitude of extracellular glutamate concentration in GLT-1 cKO mice was significantly higher than that in GLT-1 control mice ($p = .040$) (Figure 4h). These findings suggested that the faster accumulation of extracellular glutamate was due to impaired glutamate uptake by the astrocytes.

Interestingly, we also observed a significant reduction in decaying time constant in GLT-1 cKOs (black in Figure 4f) compared to GLT-1 controls ($p = .026$) (white in Figure 4f). On the other hand, the glutamate response duration was shorter in GLT-1 cKOs than in GLT-1 controls ($p = .0038$) (Figure 4i).

Taken together, these findings indicated that reduced GLT-1 increased the dynamics of glutamate changes associated with CSD.

4 | DISCUSSION

This study examined CSD in mice lacking expression of one of the genes driving glutamate transporter activity in the mouse forebrain. Our findings provide the first evidence of a critical role for glutamate transporter GLT-1 in regulating the regional susceptibility to the spreading depression. Below, we discuss the possible underlying mechanism for this effect in brain and the implications of our findings for the pathophysiology of CSD-associated neurological disorders such as migraine.

4.1 | Specificity of the glutamate transporters in the susceptibility of brain to spreading depression

Brain expresses four glutamate transporters, GLT-1, GLAST, EAAC1, and EAAT4, each of which has specific expression patterns in the mammalian brain. For example, GLT-1 is expressed ubiquitously throughout brain, while EAAT4 is localized to the cerebellum (Tanaka, 1997; Yamada et al., 1996). To address the possible contribution of any of these glutamate transporters to CSD, we limited our analysis to mice lacking gene expression for one of the three transporters expressed in cerebral cortex: GLT-1, GLAST, and EAAC1.

For GLT-1, a conventional knockout mouse showed growth retardation and died prematurely after 3 weeks of age due to lethal epileptic seizure (Tanaka, 1997), making it difficult to examine CSD in the adult mouse. Indeed, we recently reported that the subcortical but not cortical deletion of GLT-1 led to the lethal seizure (Sugimoto et al., 2018). Since we observed broad areas including subcortical structure showed a substantial reduction of GLT-1 in hGFAP-Cre; GLT-$1^{flox/flox}$ mice, it is reasonable to attribute the premature death to the increased extracellular glutamate in the subcortical areas.

In the current study, expression of Cre in a subpopulation of the astrocytes enabled us to rescue such a high mortality with conventional knockouts strategy in the current study. A recent analysis systematically examined representative Cre-expressing mouse lines for the astrocytes and showed that human GFAP promoter seems to label less than 60% of the astrocytes (Hu et al., 2020), consistent with our results. This may be accounted for by the fact that not all the astrocytes expressed GFAP as reported previously (Cahoy et al., 2008). On the other hand, it is reported that hGFAP-Cre was expressed not only in the astrocytes but in the neurons (e.g., hippocampus) (Fraser et al., 2004) and that neurons expressed GLT-1 to a lesser extent than the astrocytes (Berger, DeSilva, Chen, & Rosenberg, 2005; Torp et al., 1994). Those facts indicate that deletion of GLT-1 in the current study affect both of astrocytes and neurons in hGFAP-Cre; GLT-$1^{flox/flox}$. Taking the predominance of GLT-1 in the astrocytes over the neurons into consideration, it is still likely that the effect of GLT-1 knockout in our model on the susceptibility in spreading depression reflects the reduced uptake of extracellular glutamate into the astrocyte.

Current analysis showing significant changes in the frequency and velocity of CSD only in GLT-1 cKO, and not in mice lacking GLAST or EAAC1, clearly identified GLT-1 as a specific determinant of the susceptibility to CSD. However, this result does not necessarily exclude the possibility that the other glutamate transporters also contribute to the generation or propagation of CSD in regions outside the cerebral cortex. Indeed, GLAST may modulate the susceptibility for spreading depression via changes in the extracellular glutamate concentration in the cerebellum where the GLAST expression dominates the GLT-1 (Yamada et al., 1996). For EAAC1, it could modulate susceptibility to CSD by altering the oxidative stress status in brain. Despite its minor role in glutamate clearance, EAAC1 exerts a neuroprotective effect by its role in transporting cysteine, a precursor for neuronal antioxidant glutathione synthesis (Aoyama et al., 2006; Harada et al., 2007). A previous study showed that local tissue oxidation directly elicited CSD and associated changes in CBF in the rat brain, suggesting that EAAC1 could modulate susceptibility to CSD via changes in glutathione synthesis (Cui et al., 2003).

4.2 | Glial dysfunction with the increased susceptibility to CSD

Studies using animal models of familial hemiplegic migraine (FHM) have provided molecular insights into the understanding of CSD. Four causal genes for FHM were identified so far, and they encode proteins for ion channels (P/Q type calcium channel called CACNA1A (Ophoff et al., 1996) and voltage-dependent sodium channel SCNA1A (Dichgans et al., 2005)), subunit of ATPase ATP1A2 (De Fusco et al., 2003), and electrogenic Na^{+}-$HCO3^{-}$ cotransporter NBCe1 (SLC4A4) (Suzuki et al., 2010). Indeed, knock-in mice carrying mutations in CACNA1A or ATP1A2 identified in FHM patients had lower thresholds for CSD induction and showed higher susceptibility to CSD (Leo et al., 2011; van den Maagdenberg et al., 2004).

The higher susceptibility to CSD with mutated CACNA1A and SCNA1A could reflect the facilitated neural transmission, since a mouse orthologue of CACNA1A (Cav2.1) with mutation showed increased current density through calcium channel Cav2.1 and neurotransmitter release in neurons (van den Maagdenberg et al., 2004). It is thus likely that mutating CACNA1A and SCNA1A changes the susceptibility of the brain to CSD by altering neuronal excitability. On the other hand, other genes implicated in FHM such as ATP1A2 and SLC4A4 are expressed in astrocytes, suggesting that dysfunction in glial cells could also contribute to the altered brain susceptibility to CSD. Indeed, these two genes could modulate neural excitability by altering the functions of glial cells such as maintenance of ion homeostasis (for ATP1A2) (Leo et al., 2011) and regulation of synaptic pH (for SLC4A4) (Suzuki et al., 2010), suggesting that both neuronal and glial dysfunction could underlie susceptibility of the brain to CSD. A recent study showed the ATP1A2 mutant mice carrying human FHM2 mutation exhibited reduction of GLT-1 density and impaired clearance of extracellular glutamate (Capuani et al., 2016). Current study showing causal relationship between GLT-1 and susceptibility for CSD supported the involvement of GLT-1 in pathophysiology underlying FHM2.

In support of a role for astrocytes in CSD, the current study also showed that disrupting GLT-1 in the astrocytes had a profound effect on susceptibility to CSD via alteration of the extracellular glutamate dynamics. A critical role of GLT-1 underlying CSD is supported by a genome-wide association study (Anttila et al., 2010) that identified a significant association between migraine and a single nucleotide polymorphism (SNP) in astrocyte elevated gene-1 (AEG-1), which inhibits the promoter activity of EAAT2 encoding glutamate transporter GLT-1 in astrocytes (Kang et al., 2005). It is therefore tempting to speculate such an SNP in the AEG-1 locus reduces glutamate uptake activity in astrocytes and subsequently leads to the increased susceptibility to CSD, resulting in migraine (Noch & Khalili, 2013).

4.3 | Regulating the dynamics of extracellular glutamate concentration via GLT-1

Excessive release of glutamate is harmful for animal survival, since it leads to the synchronous discharge of neuronal activity and excitotoxic damage to the brain (Michaelis, 1998). Since GLT-1 plays a primary role in >90% of extracellular glutamate uptake (Haugeto et al., 1996; Tanaka, 1997), homozygotes of the germ-line GLT-1 knockout allele showed lethal seizure and selective neuronal degeneration in many brain regions such as hippocampus and cerebral cortex (Kiryk et al., 2008; Tanaka, 1997).

Despite the accumulating evidence supporting a role for glutamate transporters in neural excitability (Danbolt, 2001), it remains unclear how GLT-1 modulates the spatiotemporal dynamics of glutamate in the extracellular space. Our enzyme-based biosensor measured it at 4 Hz, in clear contrast to slow sampling on the minute-to-hour time scale accomplished by conventional methods such as microdialysis using high performance liquid chromatography with electrochemical detection (Hu et al., 1994). Since CSD usually does not last longer than 5 min in the intact brain, electrochemical measurement of glutamate using similar biosensors should provide deep insights into understanding the contribution of glutamate to susceptibility of the brain to CSD. Indeed, the present analysis revealed that reduced GLT-1 activity resulted in faster accumulation of the extracellular glutamate, which may be relevant to the increased susceptibility to CSD. Since both neuronal and glial cells are expected to depolarize during CSD, it is known that the GLT-1, which acts to release glutamate in the depolarized astrocytes (Szatkowski et al., 1990), contributes to the retained extracellular glutamate as indicated in the ischemic condition (Mitani & Tanaka, 2003). Due to the absence of such a reversed status of glutamate transporter activity, it is possible that extracellular glutamate levels in GLT-1 cKO mice decayed more quickly than those in GLT-1 controls.

For the measurement of the extracellular glutamate, amperometric signal could reflect not only glutamate change but the release of endogenous substances such as hydrogen peroxide despite the fine temporal resolution in the biosensor. Although the glutamate sensors we used have interference membranes that would reduce any possible signal to H_2O_2, but the membranes are not designed to specifically eliminate it. Thus, we cannot exclude the possibility that a sensor could respond to endogenous hydrogen peroxide by the current data.

More recently, fluorescence-based glutamate biosensor was developed and exhibited spatiotemporal resolution high enough to follow the CSD (Enger et al., 2015). Since this enabled simultaneous measurement of extracellular glutamate and potassium ion as well as neuronal and glial activation via intracellular calcium indicator, a combination of those techniques would be a promising approach to unravel roles of glutamate transporters in the spreading depression.

ACKNOWLEDGMENTS

The authors thank Dr David H. Gutmann for the Tg(GFAP-Cre) line, Masahiko Watanabe for the anti-GLT-1 antibody, Dr Shaheen Latif in Pinnacle Technology Inc. for technical advice, Ms Harumi Ishikubo, Masako Hidaka and Natural Science Center for Basic Research and Development of Hiroshima University for the technical assistance. This research was supported by a Grant-in-Aid for Scientific Research on Innovative Areas (KAKENHI26112010 and JP19H05723) and a Grant-in-Aid for Challenging Exploratory Research (KAKENHI-JP17K19459) from the Ministry of Education, Culture, Sports, Science and Technology (MEXT) and Program of the Network-type Joint Usage/Research Center for Radiation Disaster Medical Science to H. A., and a grant from Core Research for Evolutional Science and Technology of Japan Science and Technology Agency to K. T. A part of this study is the result of "Understanding of Molecular and Environmental Bases for Brain Health" and "Integrated Research on Depression, Dementia and Development Disorders" (JP18dm0107093h0003) performed under the Strategic Research Program for Brain Sciences by MEXT.

DATA AVAILABILITY STATEMENT

The data that support the findings of this study are available from the corresponding author upon reasonable request.

ORCID

Hidenori Aizawa https://orcid.org/0000-0002-2896-1298
Kohichi Tanaka https://orcid.org/0000-0001-6929-4228

REFERENCES

Aida, T., Yoshida, J., Nomura, M., Tanimura, A., Iino, Y., Soma, M., … Tanaka, K. K. F. (2015). Astroglial glutamate transporter deficiency increases synaptic excitability and leads to pathological repetitive behaviors in mice. *Neuropsychopharmacology*, *40*(7), 1569–1579. https://doi.org/10.1038/npp.2015.26

Anttila, V., Stefansson, H., Kallela, M., Todt, U., Terwindt, G. M., Calafato, M. S., … Palotie, A. (2010). Genome-wide association study of migraine implicates a common susceptibility variant on 8q22.1. *Nature Genetics*, *42*(10), 869–873. https://doi.org/10.1038/ng.652

Aoyama, K., Suh, S. W., Hamby, A. M., Liu, J., Chan, W. Y., Chen, Y., & Swanson, R. A. (2006). Neuronal glutathione deficiency and age-dependent neurodegeneration in the EAAC1 deficient mouse. *Nature Neuroscience*, *9*(1), 119–126. https://doi.org/10.1038/nn1609

Ayata, C. (2013). Pearls and pitfalls in experimental models of spreading depression. *Cephalalgia*, *33*(8), 604–613. https://doi.org/10.1177/0333102412470216

Ayata, C., Shin, H. K., Salomone, S., Ozdemir-Gursoy, Y., Boas, D. A., Dunn, A. K., & Moskowitz, M. A. (2004). Pronounced hypoperfusion during spreading depression in mouse cortex. *Journal of Cerebral Blood Flow & Metabolism*, *24*(10), 1172–1182. https://doi.org/10.1097/01.WCB.0000137057.92786.F3

Bajenaru, M. L., Zhu, Y., Hedrick, N. M., Donahoe, J., Parada, L. F., & Gutmann, D. H. (2002). Astrocyte-specific inactivation of the neurofibromatosis 1 gene (NF1) is insufficient for astrocytoma formation. *Molecular and Cellular Biology*, *22*(14), 5100–5113. https://doi.org/10.1128/MCB.22.14.5100-5113.2002

Berger, U. V., DeSilva, T. M., Chen, W., & Rosenberg, P. A. (2005). Cellular and subcellular mRNA localization of glutamate transporter isoforms GLT1a and GLT1b in rat brain by in situ hybridization. *The Journal of Comparative Neurology*, *492*(1), 78–89. https://doi.org/10.1002/cne.20737

Cahoy, J. D., Emery, B., Kaushal, A., Foo, L. C., Zamanian, J. L., Christopherson, K. S., … Barres, B. A. (2008). A transcriptome database for astrocytes, neurons, and oligodendrocytes: A new resource for understanding brain development and function. *Journal of Neuroscience*, *28*(1), 264–278. https://doi.org/10.1523/JNEUROSCI.4178-07.2008

Capuani, C., Melone, M., Tottene, A., Bragina, L., Crivellaro, G., Santello, M., … Pietrobon, D. (2016). Defective glutamate and K + clearance by cortical astrocytes in familial hemiplegic migraine type 2. *EMBO Molecular Medicine*, *8*(8), 967–986. https://doi.org/10.15252/emmm.201505944

Cui, W., Mizukami, H., Yanagisawa, M., Aida, T., Nomura, M., Isomura, Y., … Aizawa, H. (2014). Glial dysfunction in the mouse habenula causes depressive-like behaviors and seep disturbance. *The Journal of Neuroscience*, *34*(49), 16273–16285. https://doi.org/10.1523/JNEUROSCI.1465-14.2014

Cui, Y., Kataoka, Y., Li, Q. H., Yokoyama, C., Yamagata, A., Mochizuki-Oda, N., … Watanabe, Y. (2003). Targeted tissue oxidation in the cerebral cortex induces local prolonged depolarization and cortical spreading depression in the rat brain. *Biochemical and Biophysical Research Communications*, *300*(3), 631–636.

Danbolt, N. C. (2001). Glutamate uptake. *Progress in Neurobiology*, *65*(1), 1–105. https://doi.org/10.1016/S0301-0082(00)00067-8

de Fusco, M., Marconi, R., Silvestri, L., Atorino, L., Rampoldi, L., Morgante, L., … Casari, G. (2003). Haploinsufficiency of ATP1A2 encoding the Na+/K+ pump α2 subunit associated with familial hemiplegic migraine type 2. *Nature Genetics*, *33*(2), 192–196. https://doi.org/10.1038/ng1081

Dichgans, M., Freilinger, T., Eckstein, G., Babini, E., Lorenz-Depiereux, B., Biskup, S., … Strom, T. M. (2005). Mutation in the neuronal voltage-gated sodium channel SCN1A in familial hemiplegic migraine. *The Lancet*, *366*(9483), 371–377. https://doi.org/10.1016/S0140-6736(05)66786-4

Dreier, J. P. (2011). The role of spreading depression, spreading depolarization and spreading ischemia in neurological disease. *Nature Medicine*, *17*(4), 439–447. https://doi.org/10.1038/nm.2333

Enger, R., Tang, W., Vindedal, G. F., Jensen, V., Johannes Helm, P., Sprengel, R., … Nagelhus, E. A. (2015). Dynamics of ionic shifts in cortical spreading depression. *Cerebral Cortex*, *25*(11), 4469–4476. https://doi.org/10.1093/cercor/bhv054

Fraser, M. M., Zhu, X., Kwon, C.-H., Uhlmann, E. J., Gutmann, D. H., & Baker, S. J. (2004). Pten loss causes hypertrophy and increased proliferation of astrocytes in vivo. *Cancer Research*, *64*(21), 7773–7779. https://doi.org/10.1158/0008-5472.CAN-04-2487

Harada, T., Harada, C., Nakamura, K., Quah, H.-M. A., Okumura, A., Namekata, K., … Tanaka, K. (2007). The potential role of glutamate transporters in the pathogenesis of normal tension glaucoma. *Journal of Clinical Investigation*, *117*(7), 1763–1770. https://doi.org/10.1172/JCI30178

Haugeto, Ø., Ullensvang, K., Levy, L. M., Chaudhry, F. A., Honoré, T., Nielsen, M., … Danbolt, N. C. (1996). Brain glutamate transporter proteins form homomultimers. *Journal of Biological Chemistry*, *271*(44), 27715–27722. https://doi.org/10.1074/jbc.271.44.27715

Hu, N. Y., Chen, Y. T., Wang, Q., Jie, W., Liu, Y.-S., You, Q. L., … Gao, T. M. (2020). Expression patterns of inducible Cre recombinase driven by differential astrocyte-specific promoters in transgenic mouse lines. *Neuroscience Bulletin*, *36*(5), 530–544. https://doi.org/10.1007/s12264-019-00451-z

Hu, Y., Mitchell, K. M., Albahadily, F. N., Michaelis, E. K., & Wilson, G. S. (1994). Direct measurement of glutamate release in the brain using a dual enzyme-based electrochemical sensor. *Brain Research*, *659*(1–2), 117–125. https://doi.org/10.1016/0006-8993(94)90870-2

Kanai, Y., & Hediger, M. A. (1992). Primary structure and functional characterization of a high-affinity glutamate transporter. *Nature*, *360*(6403), 467–471. https://doi.org/10.1038/360467a0

Kang, D., Su, Z., Sarkar, D., Emdad, L., Volsky, D. J., & Fisher, P. B. (2005). Cloning and characterization of HIV-1-inducible astrocyte elevated gene-1, AEG-1. *Gene*, *353*(1), 8–15. https://doi.org/10.1016/j.gene.2005.04.006

Kiryk, A., Aida, T., Tanaka, K., Banerjee, P., Wilczynski, G. M., Meyza, K., … Danysz, W. (2008). Behavioral characterization of GLT1 (+/−) mice as a model of mild glutamatergic hyperfunction. *Neurotoxicity Research*, *13*(1), 19–30. https://doi.org/10.1007/BF03033364

Lauritzen, M. (1994). Pathophysiology of the migraine aura. *Brain*, *117*(1), 199–210. https://doi.org/10.1093/brain/117.1.199

Lauritzen, M., & Hansen, A. J. (1992). The effect of glutamate receptor blockade on anoxic depolarization and cortical spreading depression. *Journal of Cerebral Blood Flow & Metabolism*, *12*(2), 223–229. https://doi.org/10.1038/jcbfm.1992.32

Leo, L., Gherardini, L., Barone, V., de Fusco, M., Pietrobon, D., Pizzorusso, T., & Casari, G. (2011). Increased susceptibility to cortical spreading depression in the mouse model of familial hemiplegic migraine type 2. *PLoS Genetics*, *7*(6), e1002129. https://doi.org/10.1371/journal.pgen.1002129

Michaelis, E. K. (1998). Molecular biology of glutamate receptors in the central nervous system and their role in excitotoxicity, oxidative stress and aging. *Progress in Neurobiology*, *54*(4), 369–415. https://doi.org/10.1016/S0301-0082(97)00055-5

Mitani, A., & Tanaka, K. (2003). Functional changes of glial glutamate transporter GLT-1 during ischemia: An in vivo study in the hippocampal CA1 of normal mice and mutant mice lacking GLT-1. *The Journal of Neuroscience*, *23*(18), 7176–7182. https://doi.org/10.1523/JNEUROSCI.23-18-07176.2003

Noch, E. K., & Khalili, K. (2013). The role of AEG-1/MTDH/LYRIC in the pathogenesis of central nervous system disease. *Advances in Cancer Research*, *120*, 159–192. https://doi.org/10.1016/B978-0-12-401676-7.00006-1

Ophoff, R. A., Terwindt, G. M., Vergouwe, M. N., van Eijk, R., Oefner, P. J., Hoffman, S. M. G., … Frants, R. R. (1996). Familial hemiplegic migraine and episodic ataxia type-2 are caused by mutations in the Ca2+ channel gene CACNL1A4. *Cell*, *87*(3), 543–552. https://doi.org/10.1016/S0092-8674(00)81373-2

Paxinos, G., & Franklin, K. B. J. (2008). *The mouse brain in stereotaxic coordinates* (3rd ed.). Cambridge, Massachusetts: Academic Press.

Peghini, P., Janzen, J., & Stoffel, W. (1997). Glutamate transporter EAAC-1-deficient mice develop dicarboxylic aminoaciduria and behavioral abnormalities but no neurodegeneration. *The EMBO Journal*, *16*(13), 3822–3832. https://doi.org/10.1093/emboj/16.13.3822

Phillis, J. W., Ren, J., & O'Regan, M. H. (2000). Transporter reversal as a mechanism of glutamate release from the ischemic rat cerebral cortex: Studies with dl-threo-$β$-benzyloxyaspartate. *Brain Research*, *868*(1), 105–112. https://doi.org/10.1016/S0006-8993(00)02303-9

Pines, G., Danbolt, N. C., Bjørås, M., Zhang, Y., Bendahan, A., Eide, L., … Kanner, B. I. (1992). Cloning and expression of a rat brain L-glutamate transporter. *Nature*, *360*(6403), 464–467. https://doi.org/10.1038/360464a0

Rossi, D. J., Oshima, T., & Attwell, D. (2000). Glutamate release in severe brain ischaemia is mainly by reversed uptake. *Nature*, *403*(6767), 316–321. https://doi.org/10.1038/35002090

Rothstein, J. D., Martin, L., Levey, A. I., Dykes-Hoberg, M., Jin, L., Wu, D., … Kuncl, R. W. (1994). Localization of neuronal and glial glutamate transporters. *Neuron*, *13*(3), 713–725. https://doi.org/10.1016/0896-6273(94)90038-8

Somjen, G. G. (2001). Mechanisms of spreading depression and hypoxic spreading depression-like depolarization. *Physiological Reviews*, *81*(3), 1065–1096. https://doi.org/10.1152/physrev.2001.81.3.1065

Storck, T., Schulte, S., Hofmann, K., & Stoffel, W. (1992). Structure, expression, and functional analysis of a Na(+)-dependent glutamate/aspartate transporter from rat brain. *Proceedings of the National Academy of Sciences of the United States of America*, *89*(22), 10955–10959. https://doi.org/10.1073/pnas.89.22.10955

Sugimoto, J., Tanaka, M., Sugiyama, K., Ito, Y., Aizawa, H., Soma, M., … Tanaka, K. (2018). Region-specific deletions of the glutamate transporter GLT1 differentially affect seizure activity and neurodegeneration in mice. *Glia*, *66*(4), 777–788. https://doi.org/10.1002/glia.23281

Suzuki, M., van Paesschen, W., Stalmans, I., Horita, S., Yamada, H., Bergmans, B. A., … Seki, G. (2010). Defective membrane expression of the Na+-HCO3-cotransporter NBCe1 is associated with familial migraine. *Proceedings of the National Academy of Sciences of the United States of America*, *107*(36), 15963–15968. https://doi.org/10.1073/pnas.1008705107

Szatkowski, M., Barbour, B., & Attwell, D. (1990). Non-vesicular release of glutamate from glial cells by reversed electrogenic glutamate uptake. *Nature*, *348*(6300), 443–446. https://doi.org/10.1038/348443a0

Tanaka, K. (1993). Expression cloning of a rat glutamate transporter. *Neuroscience Research*, *16*(2), 149–153. https://doi.org/10.1016/0168-0102(93)90082-2

Tanaka, K. (1997). Epilepsy and exacerbation of brain injury in mice lacking the glutamate transporter GLT-1. *Science*, *276*(5319), 1699–1702. https://doi.org/10.1126/science.276.5319.1699

Torp, R., Danbolt, N. C., Babaie, E., BjØrås, M., Seeberg, E., Storm-Mathisen, J., & Ottersen, O. P. (1994). Differential expression of two glial glutamate transporters in the rat brain: An in situ hybridization study. *European Journal of Neuroscience*, *6*(6), 936–942. https://doi.org/10.1111/j.1460-9568.1994.tb00587.x

van den Maagdenberg, A. M. J., Pietrobon, D., Pizzorusso, T., Kaja, S., Broos, L. A., Cesetti, T., … Ferrari, M. D. (2004). A Cacna1a knockin migraine mouse model with increased susceptibility to cortical spreading depression. *Neuron*, *41*(5), 701–710. https://doi.org/10.1016/S0896-6273(04)00085-6

Watase, K., Hashimoto, K., Kano, M., Yamada, K., Watanabe, M., Inoue, Y., … Tanaka, K. (1998). Motor discoordination and increased susceptibility to cerebellar injury in GLAST mutant mice. *European Journal of Neuroscience*, *10*(3), 976–988. https://doi.org/10.1046/j.1460-9568.1998.00108.x

Yamada, K., Watanabe, M., Shibata, T., Tanaka, K., Wada, K., & Inoue, Y. (1996). EAAT4 is a post-synaptic glutamate transporter at Purkinje cell synapses. *Neuroreport*, *7*(12), 2013–2017. https://doi.org/10.1097/00001756-199608120-00032

Yuzawa, I., Sakadžić, S., Srinivasan, V. J., Shin, H. K., Eikermann-Haerter, K., Boas, D. A., & Ayata, C. (2012). Cortical spreading depression impairs oxygen delivery and metabolism in mice. *Journal of Cerebral Blood Flow & Metabolism*, *32*(2), 376–386. https://doi.org/10.1038/jcbfm.2011.148

Zhao, Z., Hiraoka, Y., Ogawa, H., & Tanaka, K. (2018). Region-specific deletions of the glutamate transporter GLT1 differentially affect nerve injury-induced neuropathic pain in mice. *Glia*, *66*(9), 1988–1998. https://doi.org/10.1002/glia.23452

Zhou, N., Rungta, R. L., Malik, A., Han, H., Wu, D. C., & MacVicar, B. A. (2013). Regenerative glutamate release by presynaptic NMDA receptors contributes to spreading depression. *Journal of Cerebral Blood Flow & Metabolism*, *33*(10), 1582–1594. https://doi.org/10.1038/jcbfm.2013.113

How to cite this article: Aizawa H, Sun W, Sugiyama K, et al. Glial glutamate transporter GLT-1 determines susceptibility to spreading depression in the mouse cerebral cortex. *Glia*. 2020; 1–12. https://doi.org/10.1002/glia.23874